

C. Neumann
V. Abetz
R. Stadler

Phase behavior of ABC-triblock copolymers with two inherently miscible blocks

Received: 10 June 1997
Accepted: 19 August 1997

C. Neumann¹ · V. Abetz (✉) · R. Stadler
Makromolekulare Chemie II
Universität Bayreuth
95440 Bayreuth
Germany

¹Present address:
Stockhausen GmbH
47705 Krefeld, Germany

Abstract The phase behavior of ternary poly-1,4-isoprene-block-poly-1,2-butadiene-block-polystyrene (ABC) triblock copolymers based on a compatible diblock copolymer attached to an incompatible C-block of different lengths is investigated by differential scanning calorimetry, transmission electron microscopy and dynamic mechanical analysis. It is shown that the system behaves like a binary diblock copolymer of a mixed AB-block and a microphase separated C-block.

Key words ABC-triblock copolymers – microphase separation – dynamic mechanical analysis

Introduction

In the field of binary block copolymers a lot of work has been done on the investigation of morphologies and the transition between the ordered and the disordered phase (ODT). See for example refs. [1–10]. Also the dynamics of block copolymer chains in the melt have been studied [11]. Transitions between two different ordered phases have been investigated [12–14] and theoretical descriptions of the stability region of the different morphologies including the continuous gyroid phase were given [15, 16]. When addressing the problem of microphase transitions in ternary ABC-triblock copolymers, one interesting question is whether an ABC-triblock copolymer composed of a miscible AB-diblock copolymer attached to an incompatible C-block will behave like a diblock copolymer, where the blocks A and B can be considered to be one block as a whole and C is the other block. To find an answer to this question, we studied a system with an upper

critical solution temperature, where A and B are highly compatible, i.e. where phase separation between A and B is observed only for very large molecular weights and low temperatures. From earlier studies it is well established that blends of poly-1,4-isoprene and poly-1,2-butadiene are miscible even at very high molar masses in the range 200–400 kg/mol [17]. As the product of the Flory–Huggins interaction parameter and the degree of polymerization (χN) must be 2.5 times larger for a symmetric AB-diblock copolymer than for a blend of the disconnected blocks to achieve microphase separation, it can be expected that a poly-1,4-isoprene-block-poly-1,2-butadiene diblock copolymer with molar masses in the range between 20 and 30 kg/mol for each of the blocks will be homogeneous in the experimentally available temperature range. By the attachment of an immiscible polystyrene block to such a symmetric diblock copolymer we attempted to synthesize an ABC-triblock copolymer with two mixed and one immiscible block. However, the miscibility of the two elastomer blocks may be reduced by the

presence of the immiscible block due to the stretching of the chains as a result of the repulsive interactions at the interface (Scheme 1). Thus the question whether this chain stretching dominates the strong compatibility of the two elastomer blocks or not arises. In this paper the influence of the block length of polystyrene on the phase behavior was studied by differential scanning calorimetry (DSC), transmission electron microscopy (TEM) and dynamic mechanical analysis (DMA).

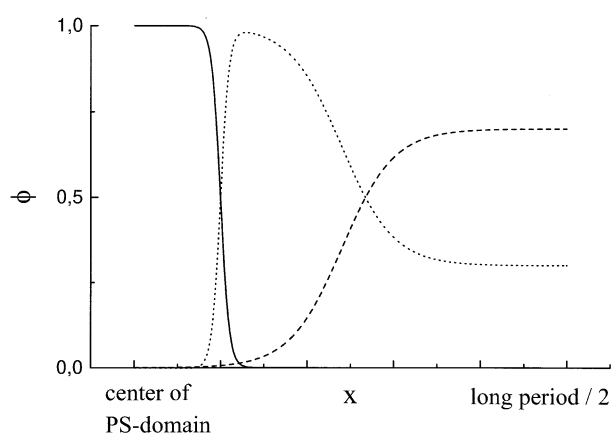
Experimental

Materials

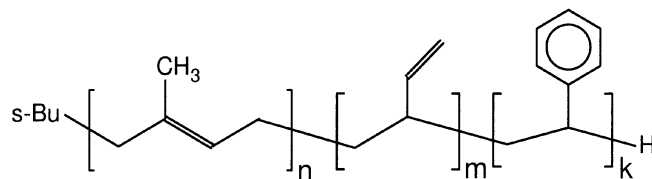
The synthesis of the poly-1,4-isoprene-block-poly-1,2-butadiene-block-polystyrene triblock copolymers (Scheme 2) by sequential anionic polymerization of isoprene, butadiene and styrene according to well-established techniques has been reported elsewhere [18, 19]. Molecular weights and polydispersity index of the precursors and the triblock copolymers were determined by size exclusion chromatography (SEC) in THF at 40 °C. All measurements were done on an instrument equipped with PLGel-columns (Bischoff). Refractive index and UV-absorption were monitored with a differential refractometer and a UV-detector (Waters). The composition and the relative amount of different microstructures in the block copolymers were determined by ^1H - and ^{13}C -NMR spectroscopy. They were obtained from CDCl_3 solutions at room temperature on a Bruker AC-200 spectrometer. The results are given in Tables 1 and 2. The following nomenclature is used for the materials: I, B and S indicate poly-1,4-isoprene, poly-1,2-butadiene and polystyrene, respectively. Subscripts denote the weight fraction and the superscript is the overall molecular weight in kg/mol.

Physical characterization

Differential scanning calorimetry measurements (DSC) were performed on a Perkin Elmer DSC 7. The T_g of P(1,4-I) and P(1,2-B) was monitored by scanning the tem-



Scheme 1 Concentration profile perpendicular to the interface between polystyrene and the elastomer blocks: (—) polystyrene, (·····) poly-1,2-butadiene, (---) poly-1,4-isoprene



Scheme 2 Structure of poly-1,4-isoprene-block-poly-1,2-butadiene-block-polystyrene triblock copolymers

perature range between -100° and 30°C after annealing the samples below T_g for several hours. The polystyrene glass transition was examined by scanning between -50° and 130°C . Scans were taken at different heating rates to allow extrapolation of the glass transition temperature to a heating rate of $0^\circ/\text{min}$.

The samples used for the dynamic mechanical analysis (DMA) were film specimen prepared by solvent casting from toluene as a good solvent for all components. The solvent was allowed to evaporate from the solution in STERIPLANTM petri dishes at room temperature. To avoid crosslinking through the influence of light and air the dishes were kept in the dark under a weak flow of nitrogen. Afterwards the samples were further dried under vacuum for one week at room temperature and for two

Table 1 Molecular weight, polydispersity index and composition of the poly-1,4-isoprene-block-poly-1,2-butadiene diblock copolymers

Diblock copolymer	M_n (PI) [kg mol ⁻¹] [Osm.]	M_n (PI) [kg mol ⁻¹] [GPC]	M_n (PB) [kg mol ⁻¹] [NMR]	M_n (app.) [kg mol ⁻¹] [GPC]	M_n [kg mol ⁻¹] [NMR]	M_w/M_n [GPC]
$I_{53}B_{47}^{45}$	24	29	21	61	45	1.04
$I_{50}B_{50}^{54}$	27	33	27	68	54	1.06
$I_{55}B_{45}^{62}$	34	41	28	79	62	1.05
$I_{50}B_{50}^{52}$	26	32	26	70	52	1.02

Table 2 Molecular weight, polydispersity index, composition and microstructure of the poly-1,4-isoprene-block-poly-1,2-butadiene-poly-styrene triblock copolymers

Triblock copolymer	M_n (PI) [kg mol ⁻¹] [Osm.]	M_n (PB) [kg mol ⁻¹] [NMR]	M_n (PS) [kg mol ⁻¹] [NMR]	M_n [kg mol ⁻¹] [NMR]	M_w/M_n [GPC]	PI-block [%]		PB-block [%]		
						1,4	3,4	1,2	1,4	Cycl.
$I_{50}B_{44}S_6^{48}$	24	21	3	48	1.07	92	8	90	2	8
$I_{45}B_{45}S_{10}^{60}$	27	27	6	60	1.03	85	15	92	—	8
$I_{46}B_{38}S_{16}^{74}$	34	28	12	74	1.03	84	16	88	6	6
$I_{37}B_{37}S_{26}^{70}$	26	26	18	70	1.03	90	10	84	8	8

days at 60 °C. Finally, they were heated to 120 °C for 3 h and cooled to room temperature under vacuum. The films were then stored in the dark at temperatures of −14 °C prior to their use for measurements.

Dynamic mechanical data were obtained with a Rheometrics RDAII rheometer equipped with a 25 mm parallel plate test fixture. Isothermal frequency sweeps were employed for the testing of the materials over a wide temperature range and isochronal temperature sweeps were conducted at four different frequencies of 0.1, 1, 10 and 100 rad/s.

The maximum strains within the linear viscoelastic regime to which the samples were deformed during isothermal tests were determined for every temperature by individual strain sweeps.

Morphological characterization

Transmission electron microscopy (TEM) was performed to investigate the morphology of the triblock copolymers. Samples were prepared from the same film specimen as for the dynamic mechanical measurements. Ultrathin sections were cut with a Reichert–Jung ultramicrotome equipped with a diamond knife at temperatures of −100 °C. The ultrathin sections were collected on gold grids and stained with OsO₄ vapor. The samples were examined with a Philips transmission electron microscope operating at 80 kV.

Results and discussion

Differential scanning calorimetry and transmission electron microscopy

In the Figs. 1A and B the DSC traces of one triblock copolymer and the corresponding poly-1,4-isoprene-block-poly-1,2-butadiene diblock copolymer are shown in the range of the glass transition temperature T_g of the elastomeric blocks and the polystyrene block, respectively. While the T_g of poly-1,4-isoprene is located at −70 °C,

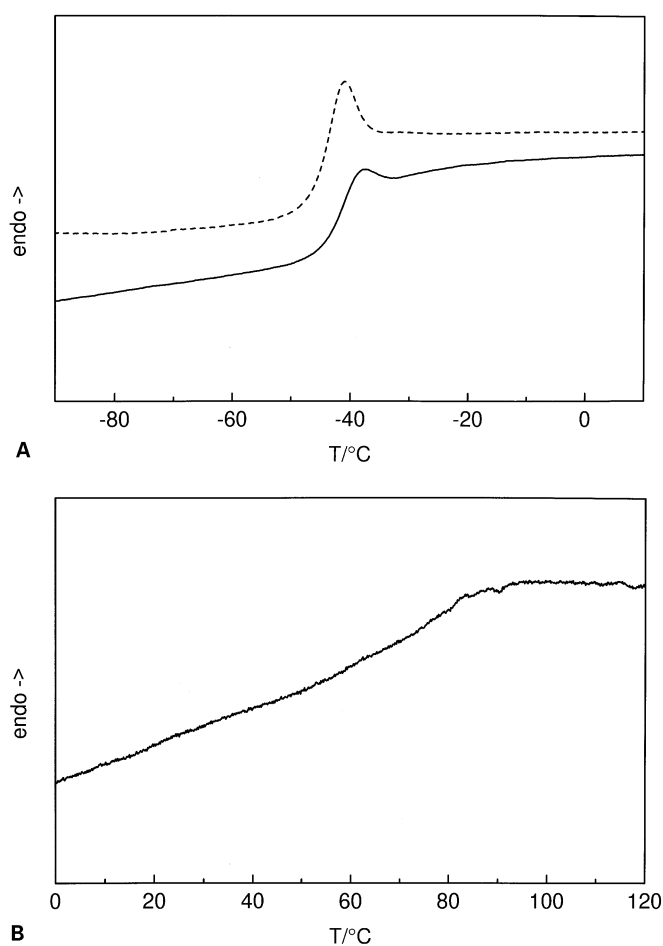


Fig. 1A DSC trace of an $I_{55}B_{45}S_{62}^{62}$ diblock (----) and an $I_{46}B_{38}S_{16}^{74}$ triblock copolymer (—) at a heating rate of 20 K/min. **B** DSC trace of $I_{46}B_{38}S_{16}^{74}$ at a heating rate of 40 K/min

T_g of the high 1,2 polybutadiene is located at ca. −10 °C. Only one glass transition is observed for the diblock copolymer at a temperature around −45 °C. The glass transition shows an enthalpy relaxation typically found for samples annealed below the glass transition temperature (the annealing procedure was performed in order to

Table 3 Glass transition temperatures of P(1,4-I), P(1,2-B) and PS in IB diblock and IBS triblock copolymers

Polymer	T_g P(1,4-I)/P(1,2-B) [°C]	Temperature range of P(1,4-I)/P(1,2-B) glass transition [°C]	ΔT_g	T_g PS [°C]
$I_{53}B_{47}^{45}$	-49	(-35)-(-50)	15	—
$I_{50}B_{50}^{44}$	-58	(-40)-(-60)	20	—
$I_{55}B_{45}^{62}$	-47	(-34)-(-54)	20	—
$I_{50}B_{50}^{52}$	-49	(-26)-(-58)	32	—
$I_{50}B_{44}S_6^{48}$	-44	(-18)-(-60)	42	18
$I_{45}B_{45}S_{10}^{60}$	-45	(-20)-(-56)	36	39
$I_{46}B_{38}S_{16}^{74}$	-43	(-16)-(-52)	36	63
$I_{37}B_{37}S_{26}^{70}$	-43	(-10)-(-52)	42	69

increase the sensitivity for the detection of two glass transition temperatures in microphase separated systems). This indicates a homogeneous mixture of the two blocks, thus confirming former results [17]. In the case of the triblock copolymer, the glass transition region is approximately two times broader as compared to the corresponding diblock copolymer. This broadening can be interpreted as a smooth gradient in the concentration profile of the two elastomer blocks due to the interface with the incompatible polystyrene block (Scheme 1). Also the glass transition region of the polystyrene block is rather broad and its T_g is significantly lower than the T_g of a homopolystyrene with a similar degree of polymerization, which indicates a certain degree of mixing at the interface between the polystyrene and elastomer domains. The results of the glass transition temperatures of all diblock and triblock copolymers are summarized in Table 3.

An increasing T_g of PS with increasing content of this block in the triblock copolymer is observed, which is basically due to the molecular weight dependence of T_g . It is noteworthy that the DSC revealed a T_g of PS for $I_{50}B_{44}S_6^{48}$ and $I_{45}B_{45}S_{10}^{60}$ although it was impossible to observe discrete polystyrene domains for these block copolymers by TEM. This is probably due to the large degree of intermixing of these short PS-blocks with the elastomeric matrix, thus leading to a too weak contrast for TEM. Sufficient contrast between the microdomains could only be realized in the polymers $I_{46}B_{38}S_{16}^{74}$ and $I_{37}B_{37}S_{26}^{70}$. Figure 2 shows a spherical morphology of the PS-phase for $I_{46}B_{38}S_{16}^{74}$ (the elastomer phase appears dark due to the staining with OsO_4). The TEM micrograph of $I_{37}B_{37}S_{26}^{70}$ in Fig. 3 reveals a cylindrical morphology of PS. A microphase separated binary diblock copolymer with volume fractions 0.16 or 0.26 of the minority component would have a spherical or a cylindrical morphology, too.

**Fig. 2** TEM micrograph of $I_{46}B_{38}S_{16}^{74}$ stained with OsO_4 (polystyrene domains appear bright)

Dynamic mechanical analysis

While we know from DSC that the two elastomeric blocks of poly-1,4-isoprene and poly-1,2-butadiene are mixed and a separated glass transition of polystyrene can be observed for all triblock copolymers studied here, TEM gave us information about the morphology at room temperature. In the following we will use DMA to investigate the microphase transition between polystyrene and the two elastomeric blocks. For diblock copolymers it has been shown before that this technique is very sensitive for the detection of the ODT [8, 9, 20].

Figures 4A and B show the temperature dependence of the storage modulus and the loss tangent of $I_{50}B_{44}S_6^{48}$ for 4 different frequencies, respectively. In Fig. 4A the transition from the glass into the rubbery plateau is shown and also the transition to the terminal flow region. The observed behavior is similar to amorphous entangled homopolymers. In Fig. 4B a maximum in the loss tangent $\tan \delta$ can be seen for the highest frequency at ca. -10°C , which is related to the dynamic glass transition of the elastomeric blocks. For all frequencies $\tan \delta$ increases monotonically vs higher temperatures indicating flow. In Fig. 4C the storage modulus is shown as a function of the loss modulus (Han-plot) for different temperatures. At



Fig. 3 TEM micrograph of $I_{37}B_{37}S_{20}^{70}$ stained with OsO_4 (polystyrene domains appear bright)

storage moduli larger than 1 MPa the system is vitrifying. Between 1 and 0.1 MPa the system is in the rubbery plateau and below that a linear relationship between G' and G'' is observed with a slope of 2. This reflects the typical frequency dependence in the terminal flow region for a homogeneous polymer of both G' ($G' \propto \omega^2$) and G'' ($G'' \propto \omega^1$). From these dynamic mechanical properties we conclude that in the case of $I_{50}B_{44}S_6^{48}$, the PS block mixes immediately with the P(1,4-I)/P(1,2-B) phase above the T_g of polystyrene. T_g of polystyrene is somehow hidden in the rubbery plateau of the elastomeric blocks, which may be the reason for the slight spread of the data in the rubbery region of the Han-plot (for a perfectly homogeneous material one master-curve would be expected for all temperatures).

Figures 5A–C show the analogous data for $I_{45}B_{45}S_{10}^{60}$. For this system in the storage modulus a second plateau is observed right after the rubber plateau of the elastomeric blocks. This second plateau is due to the still glassy polystyrene domains. The inflection point between the rubber and the second plateau of the storage modulus gives rise to a broad maximum in $\tan \delta$ in Fig. 5B (at ca. 25 °C for 0.1 rad/s). The loss modulus (not shown) does not show any maximum related to this maximum. As in the case of $I_{50}B_{44}S_6^{48}$ for the highest frequency a maximum in $\tan \delta$

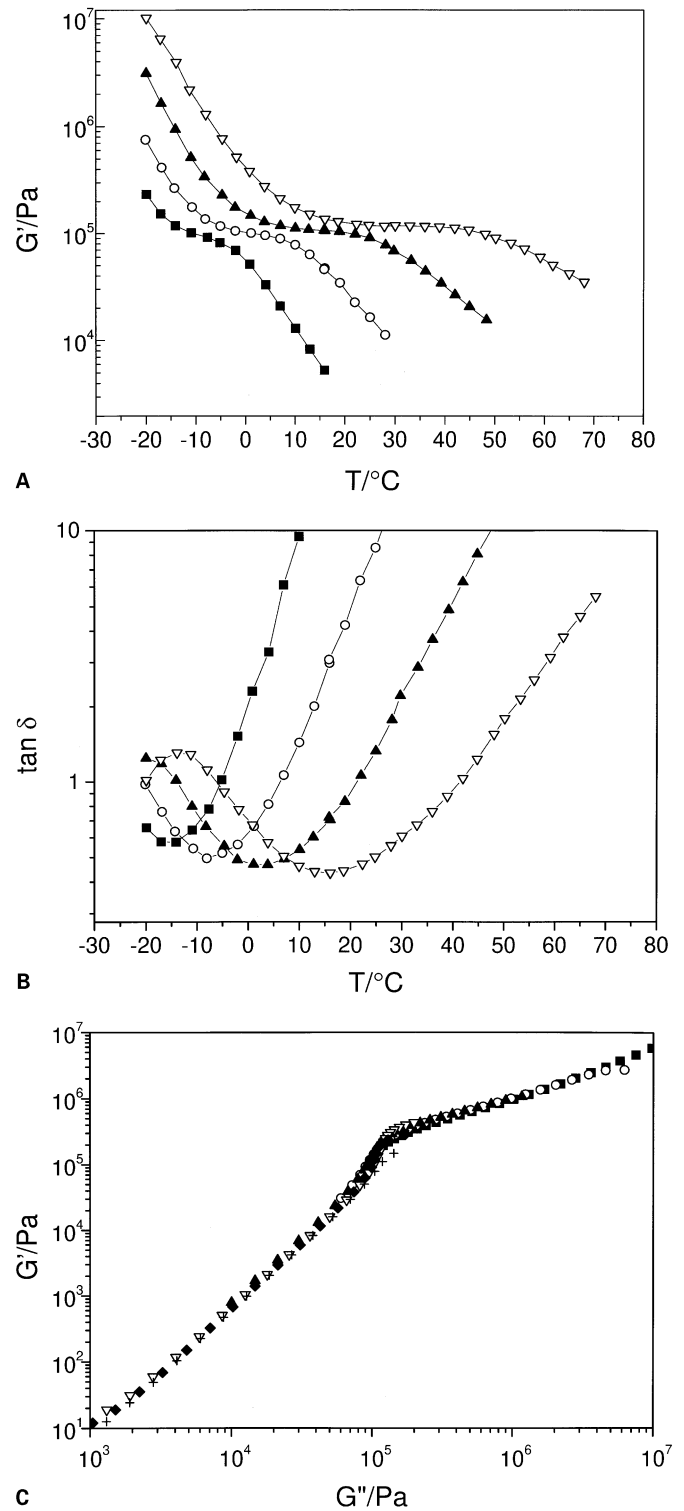
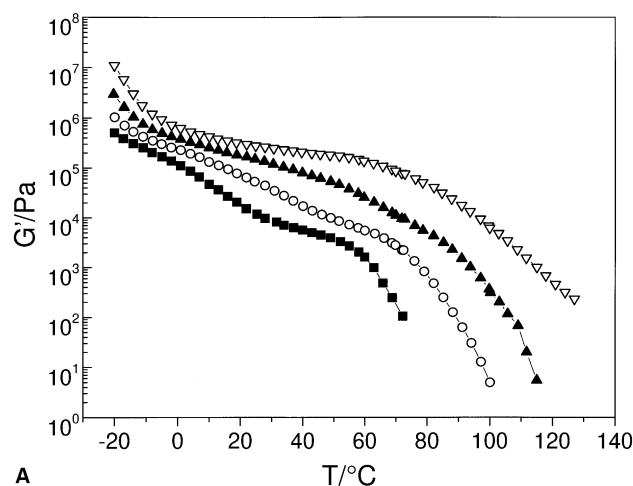


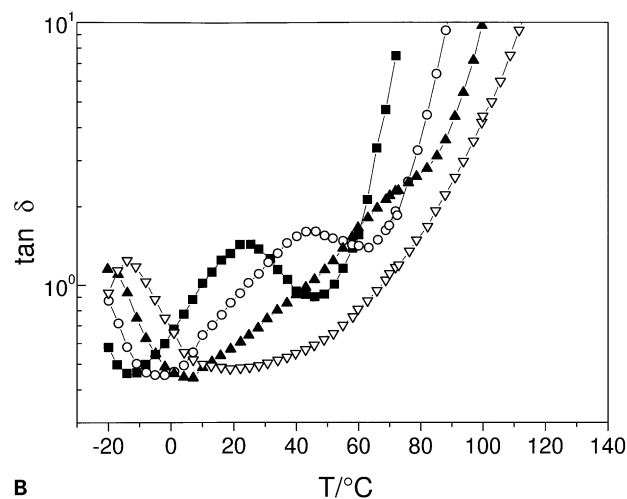
Fig. 4A Storage modulus of $I_{50}B_{44}S_6^{48}$ as a function of temperature for: (■) 0.1 rad/s, (○) 1 rad/s, (▲) 10 rad/s and (▽) 100 rad/s. **B** Loss tangent of $I_{50}B_{44}S_6^{48}$ as a function of temperature for: (■) 0.1 rad/s, (○) 1 rad/s, (▲) 10 rad/s and (▽) 100 rad/s. **C** Han plot of $I_{50}B_{44}S_6^{48}$ for different temperatures for: (■) -20 °C, (○) -10 °C, (▲) 0 °C, (▽) 20 °C, (◆) 40 °C, (+) 60 °C, (×) 80 °C

related to the glass transition of the elastomeric blocks is found at ca. -10°C . Above T_g of polystyrene G' drops off in a similar way as for a homopolymer, indicating again the mixing of the PS-block with the elastomeric blocks right above the T_g of PS. This also can be seen from the typical increase of $\tan\delta$ at high temperatures. Also the maximum in $\tan\delta$ assigned to the inflection point of G' between the rubber and this second plateau vanishes for the highest frequency. At 100 rad/s the rubber plateau is extended at least up to the glass transition temperature of PS and above T_g of PS the system seems to become homogeneous.

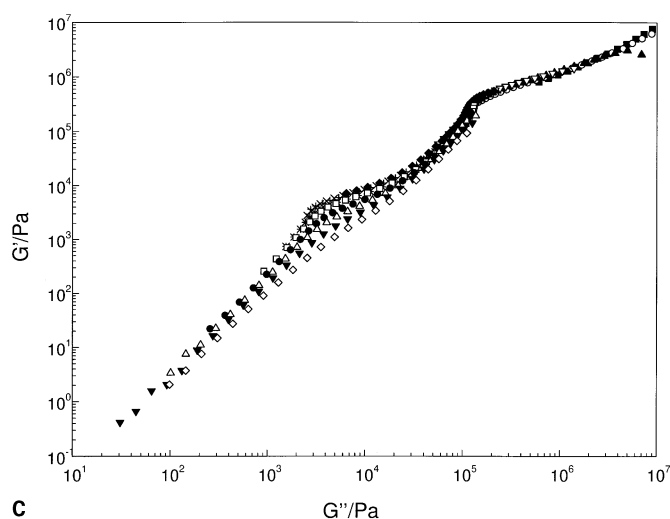
In the Han plot (Fig. 5C) one observes a spreading of the data in the range of ca. 1 kPa up to 10 kPa for temperatures up to 80°C , which is due to the glass transition of PS. Above 80°C again a slope of 2 is observed, indicating a homogeneous melt in the terminal flow region. Investigations of Schwab and Stühn [5] on a poly-1,4-isoprene-block-polystyrene diblock copolymer with an overall



A



B



C

Fig. 5A Storage modulus of $I_{45}B_{45}S_{10}^{60}$ as a function of temperature for: (■) 0.1 rad/s, (○) 1 rad/s, (▲) 10 rad/s and (▽) 100 rad/s. **B** Loss tangent of $I_{45}B_{45}S_{10}^{60}$ as a function of temperature for: (■) 0.1 rad/s, (○) 1 rad/s, (▲) 10 rad/s and (▽) 100 rad/s. **C** Han plot of $I_{45}B_{45}S_{10}^{60}$ for different temperatures for: (■) -30°C , (○) -20°C , (▲) -10°C , (▽) 0°C , (◆) 20°C , (+) 35°C , (×) 42.5°C , (*) 50°C , (□) 57.5°C , (●) 65°C , (Δ) 70°C , (▼) 80°C , (◇) 90°C

molecular weight of 46 000 g/mol and a volume fraction of 0.11 for polystyrene displayed a much higher ODT at 120°C . This difference indicates a weaker incompatibility between poly-1,4-isoprene-block-poly-1,2-butadiene towards polystyrene as compared to poly-1,4-isoprene towards polystyrene.

In comparison with $I_{45}B_{45}S_{10}^{60}$, the temperature-dependent dynamic mechanical measurements of $I_{46}B_{38}S_{16}^{74}$ look rather different at high temperatures, since a terminal decay in the storage modulus cannot be observed, but the curves seem to end in a plateau within the experimental temperature range (Fig. 6A). This observation suggests a persistent phase separation between the polystyrene block and the elastomer blocks at temperatures well above T_g of the polystyrene block. As in $I_{45}B_{45}S_{10}^{60}$, the broad maximum in $\tan\delta$ which is related to the transition between the rubber and a second plateau is showing a significant frequency dependence (Fig. 6B). The maximum is more pronounced than in $I_{45}B_{45}S_{10}^{60}$. In the 0.1 and 100 rad/s curves a separate relaxation which is attributable to the PS glass transition can be seen as a high-temperature respectively low-temperature shoulder of the broad maximum in the $\tan\delta$ (between 60°C and 70°C).

In Fig. 6C a significant spread of the data of G' as a function of G'' is seen between 1 and 10 kPa. This is again due to the glass transition of the polystyrene block. However, above that glass transition no terminal flow behavior

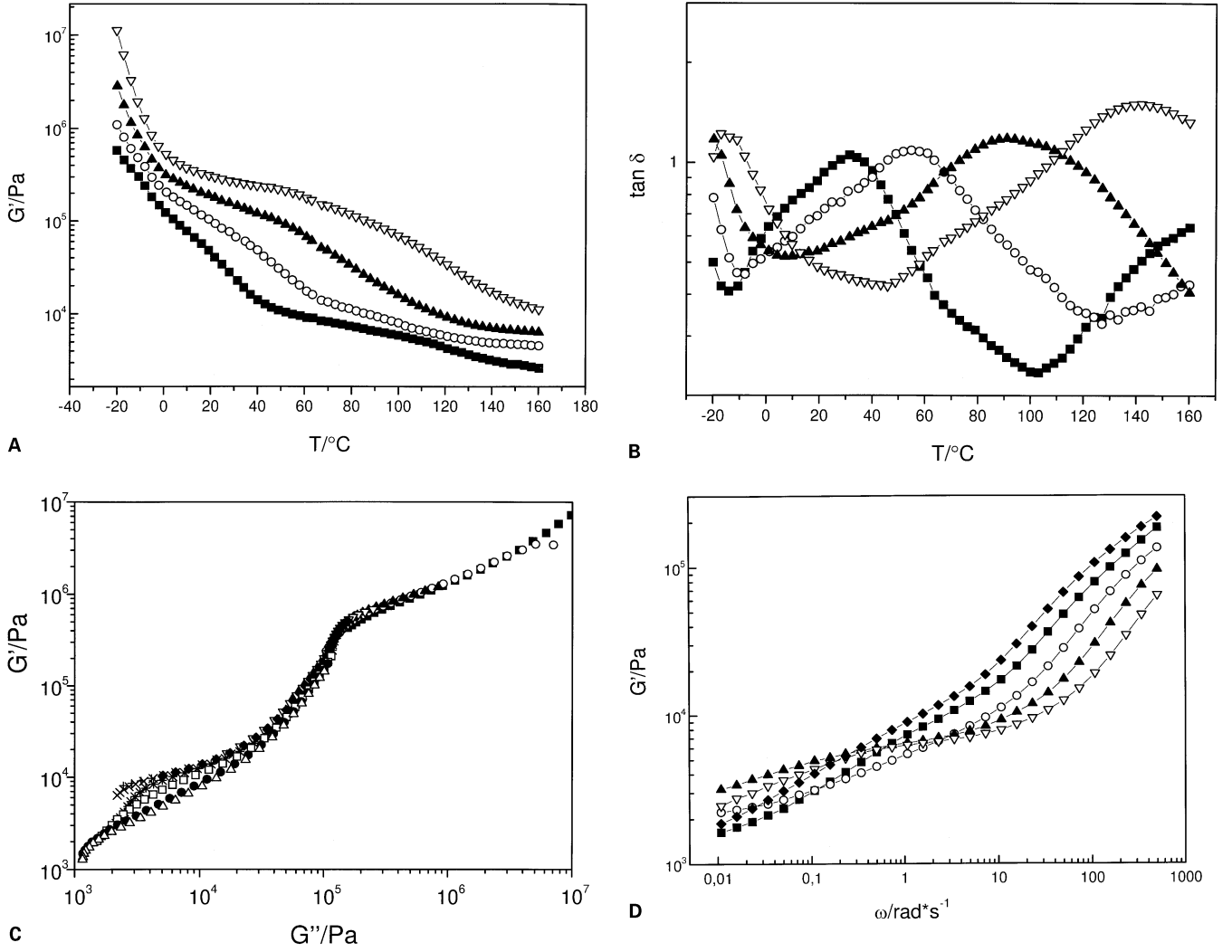


Fig. 6A Storage modulus of $I_{46}B_{38}S_{16}^{74}$ for different temperatures for: (■) 0.1 rad/s, (○) 1 rad/s, (▲) 10 rad/s and (▽) 100 rad/s. **B** Loss tangent of $I_{46}B_{38}S_{16}^{74}$ as a function of temperature for: (■) 0.1 rad/s, (○) 1 rad/s, (▲) 10 rad/s and (▽) 100 rad/s. **C** Han plot of $I_{46}B_{38}S_{16}^{74}$ for different temperatures for: (■) -20°C , (○) -10°C , (▲) 5°C , (▽) 20°C , (◆) 35°C , (+) 50°C , (×) 65°C , (*) 80°C , (□) 90°C , (●) 100°C , (△) 110°C . **D** Storage modulus of $I_{46}B_{38}S_{16}^{74}$ as a function of frequency for: (■) 100°C before heating, (○) 120°C , (▲) 135°C , (▽) 150°C , (◆) 100°C after heating

is observed (the slope is less than 1). Only for very low values of the moduli a larger slope might indicate the neighborhood to the order disorder transition. To clarify this, in Fig. 6D isothermal plots of the storage modulus are plotted as function of the frequency for high temperatures. While for large frequencies G' drops with increasing temperature, there is a crossover at lower frequencies. At 135°C and 150°C larger values of G' for frequencies below ca. 3 rad/s are measured than for 100°C . Measuring again at 100°C after heating up to 150°C nearly reproduces the curve of the measurement at 100°C before heating up to 150°C . Cooling the sample at 20° for 3 h and reheating it to 100°C reproduces the same G' values during an isother-

mal frequency sweep as during the first measurement at 100°C (not shown). Therefore, it can be concluded that the increase of the modulus at 135°C and 150°C is not due to the thermally-induced crosslinking of the double bonds of P(1,4-I) and P(1,2-B). We think that the increasing G' values at elevated temperatures are due to the onset of mixing between the PS phase and the P(1,4-I)/P(1,2-B) phase. The interfacial region between PS domains and the P(1,4-I)/P(1,2-B) broadens when approaching the ODT. As PS has a much higher segmental friction coefficient than P(1,4-I) and P(1,2-B) the interpenetration enhances the overall frictional resistance to shear deformation and therefore results in a higher storage modulus. This effect is

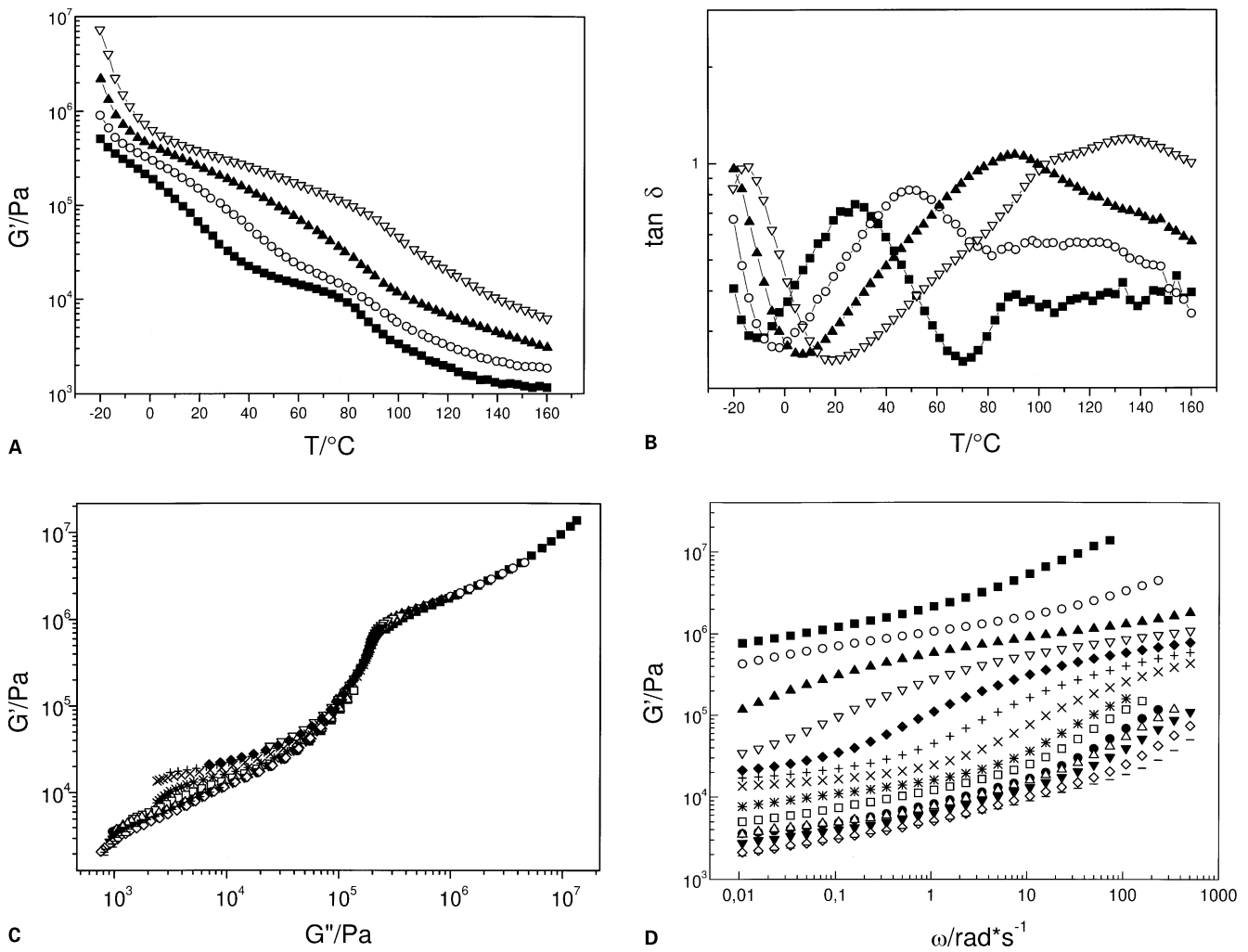


Fig. 7A Storage modulus of $I_{37}B_{37}S_{26}^{70}$ as a function of temperature for: (■) 0.1 rad/s, (○) 1 rad/s, (▲) 10 rad/s and (▽) 100 rad/s. **B** Loss tangent of $I_{37}B_{37}S_{26}^{70}$ as a function of temperature for: (■) 0.1 rad/s, (○) 1 rad/s, (▲) 10 rad/s and (▽) 100 rad/s. **C** Han plot of storage modulus of $I_{37}B_{37}S_{26}^{70}$ as a function of frequency for: (■) -20 °C, (○) -10 °C, (▲) 5 °C, (▽) 20 °C, (◆) 35 °C, (+) 50 °C, (×) 65 °C, (*) 80 °C, (□) 90 °C, (●) 100 °C, (△) 110 °C, (▼) 120 °C, (◇) 135 °C, (-) 150 °C. **D** Storage modulus of $I_{37}B_{37}S_{26}^{70}$ as a function of frequency for: (■) -20 °C, (○) -10 °C, (▲) 5 °C, (▽) 20 °C, (◆) 35 °C, (+) 50 °C, (×) 65 °C, (*) 80 °C, (□) 90 °C, (●) 100 °C, (△) 110 °C, (▼) 120 °C, (◇) 135 °C, (-) 150 °C

opposed to some extent by the increasing temperature, since the values of G' at 135 °C are higher than at 150 °C in the low-frequency region.

Up to 50 °C the block copolymer $I_{37}B_{37}S_{26}^{70}$ shows a behavior very similar to $I_{46}B_{38}S_{16}^{74}$ (Figs. 7A–C). As the frequency in these measurements is increased, the plateau in G' above 0 °C is extended to higher temperatures. Therefore, the decay in G' , which appears at 20 °C in the sweep with 0.1 rad/s and which is characterized by the broad maximum in the loss tangent, moves to 40 °C in the 1.0 rad/s experiment (Fig. 7A). As a result of this shift to higher temperature, the decrease of G' at 80 °C due to the glass transition of polystyrene is hidden in the 10 rad/s

measurement. At 0.1, 1.0 and 100 rad/s T_g (PS) can be identified by the decrease of G' and a maximum or shoulder in $\tan \delta$ in the region of 90 °C.

The Han-plot of this polymer looks very similar to the one of $I_{46}B_{38}S_{16}^{74}$ (Fig. 7C). To investigate the question, whether the ODT for this system is at least close to the highest measurement temperature used (150 °C), measurements at even higher temperatures could not be performed, due to problems with the thermal stability of this material. In Fig. 7D isothermal plots of the storage modulus as a function of frequency are shown for all temperatures. In comparison to $I_{46}B_{38}S_{16}^{74}$ no significant cross-over of G' is observed for higher temperatures. Also

the slope of G' as a function of frequency at low frequencies remains constant for temperatures between 110 °C and 150 °C ($G' \propto \omega^{0.1}$). Thus the system is further away from the ODT as compared to $I_{46}B_{38}S_{16}^{74}$, which is understandable due to the larger polystyrene block.

Conclusion

Ternary ABC-triblock copolymers based on poly-1,4-isoprene-block-poly-1,2-butadiene-block-polystyrene behave like diblock copolymers consisting of a mixed poly-1,4-isoprene/poly-1,2-butadiene block segregated from polystyrene. For the systems studied here no microphase separation between the two elastomer blocks due to the repulsive interaction at the interface with the polystyrene domains could be observed. The presence of the polystyrene block causes a broadening of the glass transition of the mixed elastomer phase, which indicates a smooth concentration gradient of the elastomer blocks within their domains rather than a stronger separation between them leading to two separated glass transitions. Also the glass transition of polystyrene is broadened and shifted to lower temperatures as compared to homopolystyrene of a sim-

ilar degree of polymerization. This indicates a certain degree of mixing with the elastomer. Thus the system is not really strongly segregated (with a sharp interface). The onset of the terminal relaxation of the elastomer chains remains unchanged for the different block lengths of polystyrene investigated. However, in the case that polystyrene and the elastomer blocks stay microphase separated up to higher temperatures, a second plateau at higher temperatures after the rubber plateau is found for the dynamic storage modulus. This plateau is due to a melt containing glassy or liquid microphase separated polystyrene domains. For the triblock copolymers with short polystyrene blocks an order-disorder transition temperature was found upon heating, thus this ternary system shows an upper critical solution temperature. This behavior is similar to poly-1,4-isoprene-block-polystyrene diblock copolymers. While the ternary triblock copolymers studied here behave like binary diblock copolymers, the situation changes significantly after hydrogenation of the two elastomer blocks. This will be discussed in a future publication [21].

Acknowledgements This work was supported by the BMBF and by the BASF AG through the joint project 03M40861 and by the DFG through SFB 262, project S-14.

References

1. Bates FS, Fredrickson GH (1990) *Ann Rev Phys Chem* 41:525
2. Förster S, Khandur AK, Zhao J, Bates FS, Hamley IW, Ryan AJ, Bras W (1994) *Macromolecules* 27:6922
3. Rosedale JH, Bates FS, Almdal K, Mortensen K, Wignall GD (1995) *Macromolecules* 28:1429
4. Colby RH (1996) *Current Opinion Colloid Interface Sci* 1:454
5. Schwab M, Stühn B (1996) *Phys Rev Lett* 76:924
6. Schulz MF, Bates FS, Almdal K, Mortensen K (1994) *Phys Rev Lett* 73:86
7. Hamley IW, Gehlsen MD, Khandur AK, Koppi KA, Rosedale JH, Schulz MF, Bates FS, Almdal K, Mortensen K (1995) *J PhysII (Fr)* 4:2161
8. Han CD, Baek DM, Kim JK (1990) *Macromolecules* 23:561
9. Gehlsen MD, Almdal K, Bates FS (1992) *Macromolecules* 25:939
10. Kornfield JA, Krishnamoorti R, Gupta VK, Chen ZR, Smith SD, Ashraf A (1995) *Polymer Preprints* 36(1):172
11. Dalvi MC, Lodge TP (1994) *Macromolecules* 27:3487
12. Sakurai S, Kawada H, Hashimoto T, Fetters LJ (1993) *Macromolecules* 26:5796
13. Hajduk DA, Gruner SM, Rangarajan P, Register RA, Fetters LJ, Honeker C, Albalak RJ, Thomas EL (1994) *Macromolecules* 27:490
14. Hajduk DA, Harper PE, Gruner SM, Honeker CC, Kim G, Thomas EL, Fetters LJ (1994) *Macromolecules* 27:4063
15. Matsen MW, Bates FS (1996) *Macromolecules* 29:1091
16. Erukhimovich IYa (1996) *JETP Lett* 63:460
17. Roland CM, Trask CA (1989) *Macromolecules* 22:256
18. Neumann C, Abetz V, Stadler R (1996) *Polym Bull* 36:43
19. Halasa AF, Lohr DF, Hall JE (1981) *J Polym Sci Polym Chem Ed* 19:1357
20. Han CD, Kim J (1987) *J Polym Sci Polym Phys Ed* 25:1741
21. Neumann C, Loveday DR, Abetz V, Stadler R, in preparation